Colloidal synthesis of nanocrystals and nanocrystal superlattices

by C. B. Murray
Shouheng Sun
W. Gaschler
H. Doyle
T. A. Betley
C. R. Kagan

This paper provides an overview of the synthetic techniques used to prepare colloidal nanocrystals (NCs) of controlled composition, size, shape, and internal structure and the methods for manipulation of these materials into ordered NC assemblies (superlattices). **High-temperature solution-phase synthesis** (100-300°C) is followed by size-selective separation techniques in the preparation of monodisperse NC samples tunable in size from \sim 1 to 15 nm in diameter with <5% standard deviation. Each NC consists of a crystalline inorganic core coordinated by an organic monolayer. These monodisperse NC samples enable systematic studies of structural, electronic, magnetic, and optical properties of materials as a function of size evolution from molecular species (<100 atoms) to bulk solids (>100 000 atoms). We illustrate size-dependent properties for magnetic materials using Co and for semiconducting materials using PbSe. These NC samples are sufficiently uniform in size to self-assemble into close-packed, ordered NC superlattices, also known as colloidal crystals.

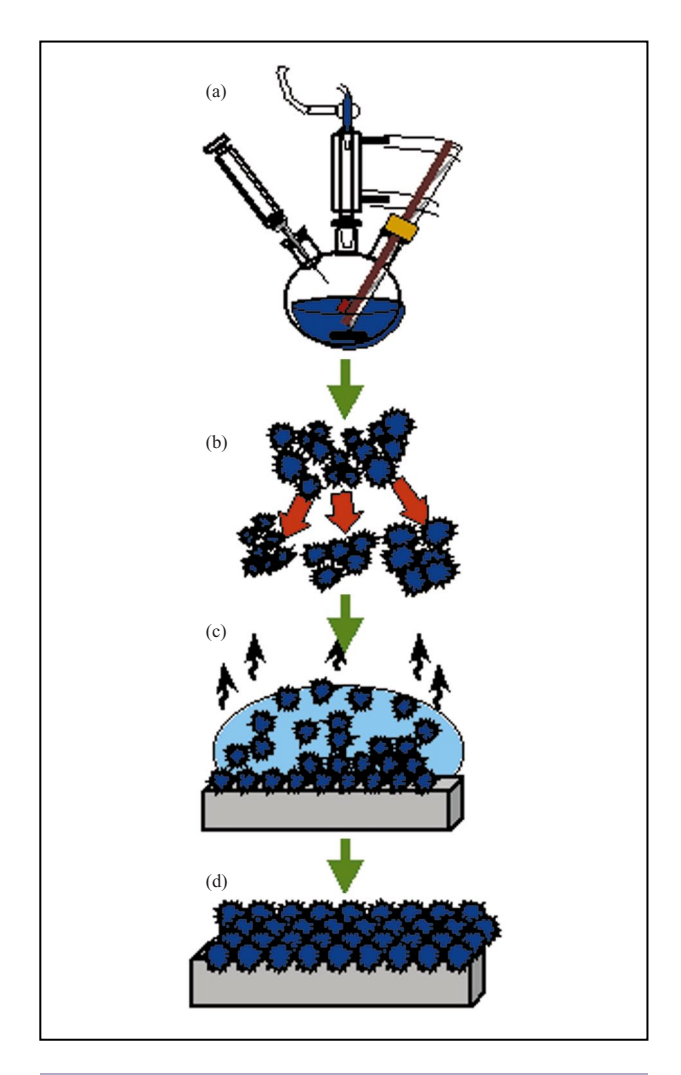
Introduction

Cooperative interactions between atoms in condensed matter produce the physical properties that are recognized as characteristic of bulk solids. The natural length scale of many of these physical phenomena lies between 1 and 15 nm (10² and 10⁵ atoms). In nanometer-scale structures, finite size effects give rise to novel electronic, magnetic, optical, and structural properties. The desire to identify, understand, and exploit the size-dependent properties of materials at the nanometer scale motivates the study of monodisperse nanometer-scale crystals, known as nanocrystals (NCs). For example, magnetic [1–5] and semiconductor [6–9] NCs exhibit strong size-dependent properties that may provide insight into the scaling limits of magnetic storage and microelectronics, key components in information technology.

Preparation of NC samples that are uniform in composition, size, shape, internal structure, and surface chemistry is essential to successfully mapping their size-dependent materials properties. High-temperature solution-phase synthesis provides a method of preparing such uniform NC samples for a variety of metals [5, 10] and semiconductors [9, 11]. Each NC in a sample consists of an inorganic crystalline core surrounded by an organic monolayer. Structural and chemical probes of the

©Copyright 2001 by International Business Machines Corporation. Copying in printed form for private use is permitted without payment of royalty provided that (1) each reproduction is done without alteration and (2) the Journal reference and IBM copyright notice are included on the first page. The title and abstract, but no other portions, of this paper may be copied or distributed royalty free without further permission by computer-based and other information-service systems. Permission to republish any other portion of this paper must be obtained from the Editor.

0018-8646/01/\$5.00 © 2001 IBM



Schematic representation of the synthetic procedures to (a) synthesize NC samples by high-temperature solution-phase routes, (b) narrow the NC sample size distribution by size-selective precipitation, (c) deposit NC dispersions that self-assemble, and (d) form ordered NC assemblies (superlattices).

inorganic core and the organic monolayer are necessary to develop structural models of NC samples. Only with careful characterization can the size-dependent magnetic, optical, and electronic properties characteristic of the NCs in the sample be uncovered.

These NC samples may then be used as the building blocks for close-packed NC solids. The organic monolayer coordinating each NC surface enables uniform NC samples, under controlled conditions, to self-assemble into NC superlattices [5, 12]. These hybrid organic–inorganic materials combine the unique properties characteristic of the "individual" NC with new collective properties arising from interactions between neighboring NCs in the

superlattice [13, 14]. Controlling the size and composition of the NCs and the length and chemical functionality of the organic monolayer allows the properties of the individual NC building blocks and the collective properties of the NC superlattices to be engineered.

General synthesis of monodisperse inorganic NCs and NC superlattices

A general scheme for preparing monodisperse NC samples (with <5% standard deviation in size) requires a single, temporally short nucleation event followed by slower growth on the existing nuclei. This may be achieved by rapid addition of reagents into a reaction vessel containing a hot, coordinating solvent [Figure 1(a)] [11]. The temperature of the solution is sufficient to decompose the reagents, forming a supersaturation of species in solution that is relieved by nucleation of NCs. Upon nucleation the concentration of these species in solution drops below the critical concentration for nucleation, and further material can only add to the existing nuclei.

An alternative synthetic approach involves mixing the reagents in a vessel at a temperature low enough to preclude any appreciable reaction. A controlled ramp of the solution temperature accelerates the chemical reaction and produces the requisite supersaturation, which is then relieved by a burst of nucleation. As long as the temperature is adjusted to keep the rate at which the reagents react less than or equal to the rate at which material adds to the existing nuclei, the supersaturated state is never revisited and no new nuclei form. In either approach, the size distribution of the NC sample is limited primarily by the short time interval in which the nuclei form and begin to grow.

The systematic adjustment of the reaction conditions—time, temperature, and concentration and chemistry of reagents and surfactants—can be used to control NC size and thus prepare a size series of NC samples. In general, NC size increases with increasing reaction time, as more material adds to NC surfaces, and with increasing temperature, as the rate of addition of material to the existing nuclei increases. Many systems also exhibit a second, distinct, growth stage known as Ostwald ripening, in which the high surface energy of the smaller NCs promotes their dissolution, while material is redeposited on the larger NCs. The average NC size increases over time, with a compensating decrease in NC number. Higher solution temperatures enhance Ostwald ripening, also leading to larger average NC size.

Tailoring the ratio of the concentration of reagents to that of surfactants provides another control over NC size, since high stabilizer-to-reagent concentrations favor the formation of more small nuclei initially and thus a smaller NC size [10]. The chemistry of the surface agent can also be chosen to control NC size. During NC growth, the

surfactants in solution adsorb reversibly to the surfaces of the NCs, providing a dynamic organic shell (capping layer) that stabilizes the NCs in solution and mediates their growth. Surfactants that bind more tightly to the NC surface or larger molecules providing greater steric hindrance (bulkier surfactants) slow the rate of materials addition to the NC, resulting in smaller average NC size. For example, bulkier trioctylphosphines provide larger steric hindrance than more compact tributylphosphines, slowing NC growth. An effective strategy involves using a pair of surface agents of which one binds tightly to the NC surface, hindering growth, and the other is less tightly bound, permitting rapid growth. For example, judicious adjustment of the ratio of carboxylic acid (tightly bound) and alkylphosphine (weakly bound) stabilizers allows the growth rate and therefore the size of the NCs to be controlled (see discussion of Co NCs below).

Alternatively, the size of NC samples may also be increased by supplying additional reagent feedstock to a solution of growing NCs. As long as the rate of feedstock addition does not exceed the rate of material addition to the NCs, the NCs continue to grow without creation of new nuclei. This controlled addition of reagents can be optimized to narrow or "focus" the NC size distribution as material adds to all NCs at nearly equal rates and produces an initial variation in NC size that is small compared to the larger, final size of the NCs [15].

When the NC sample reaches the desired size, further growth is arrested by cooling the solution. The NC dispersions are stable if the interaction between the capping groups and the solvent is favorable, providing an energetic barrier to counteract the van der Waals and magnetic (for magnetic materials) attractions between NCs. The NCs are then isolated from their growth solution. Introducing a nonsolvent that is miscible with the first solvent but has an unfavorable interaction with the capping groups (hence "nonsolvent") reduces the barrier to aggregation and destabilizes the NC dispersion, causing their flocculation. Centrifuging the resulting turbid suspension allows the solvent to be decanted and powders of the NCs to be isolated. These powders consist of the desired NCs and their intimate organic capping layer and can be redispersed in a variety of solvents.

The general synthetic approaches described in this paper can be optimized to yield size distributions $\sigma \lesssim 10\%$ in diameter, which can then be further narrowed to $\sigma \lesssim 5\%$ through size-selective precipitation, as depicted in Figure 1(b). Size-selective precipitation involves the slow titration of a nonsolvent into the dispersion to bring about its partial flocculation [11, 16]. Since the largest NCs experience the greatest attractive forces, they aggregate first. If the dispersion is allowed to flocculate only partially, filtering or centrifuging the suspension isolates a precipitate enriched in the larger NCs and leaves the

smaller NCs dispersed in the supernatant, which is then decanted. Additional nonsolvent may be added to the supernatant to isolate a second fraction of smaller NCs. The precipitates isolated can in turn be redispersed in a solvent and subjected recursively to this gentle destabilization/redispersion procedure to further narrow the sample size distribution. Narrower initial size distributions allow the desired σ value to be attained with fewer stages of size-selective precipitation and thus provide higher yields.

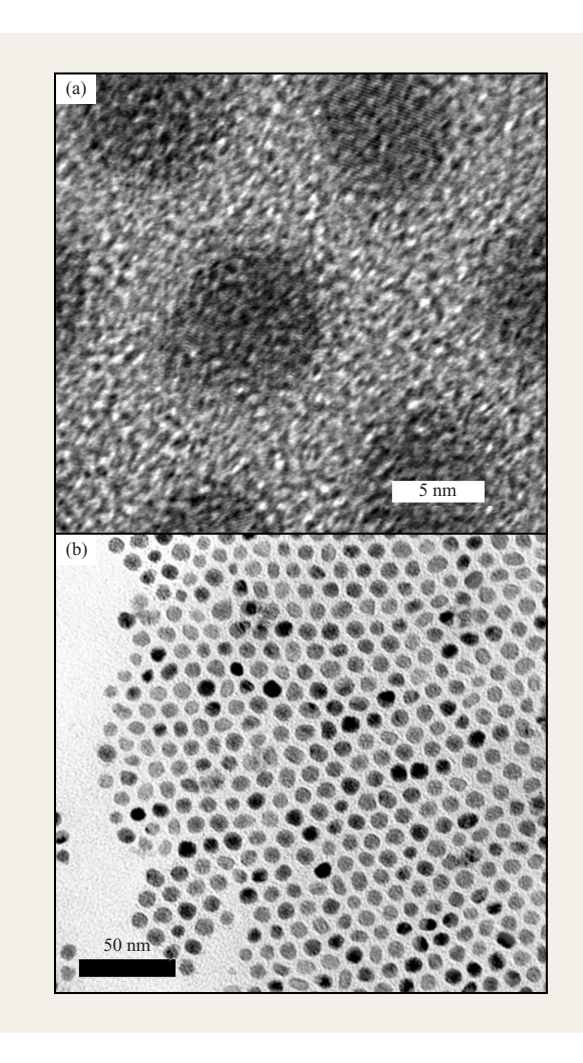
The monolayer of organic capping groups bound to the NC surface can be exchanged with other competing capping groups. Repeated exposure of the NCs to an excess of the competing capping groups, followed by precipitation and redispersion in fresh solvent, isolates cap-exchanged NCs [9]. This process allows the length and chemical functionality of the organic capping layer to be precisely adjusted.

NC samples with narrow size distributions can be deposited from solvents to assemble into NC superlattices (also known as colloidal crystals), as depicted in **Figures 1(c)** and **1(d)**. The solvent used to deposit the NC superlattices is selected for its polarity and for its boiling point. The solvent polarity is chosen so that the interaction between NCs will become mildly attractive as the solvent evaporates and the dispersion becomes more concentrated. The boiling point of the solvent is selected to permit the NCs enough time to find equilibrium lattice sites before the solvent evaporates on the growing NC superlattice.

The NC superlattices formed are waxy solids held together by weak van der Waals and dipolar magnetic attractions. They may be made more rigid and robust by selecting organic capping groups that will cross-link upon exposure to radiation (UV or electron beam) or upon heating. For example, heating an NC superlattice to ~300°C under one atmosphere of an inert gas, such as argon, cross-links some organic capping groups, forming an amorphous carbon matrix between NCs in the superlattice [5, 17]. In many NC superlattice systems, heating under vacuum leads to desorption of the organic capping groups and controlled sintering of the NCs into a fully inorganic solid [9].

Nanocrystal magnets: Monodisperse cobalt NCs

The synthesis of metal colloids has been studied for more than a century, and yet the number of preparations yielding a size series of monodisperse transition metal NC samples remains relatively small [18]. Cobalt serves as a model system for magnetic scaling in materials because its low to moderate crystal anisotropy allows the effects of size, shape, internal crystal structure, and surface anisotropy to be observed in a single system. Synthetic



(a) High-resolution TEM image of 7-nm hcp Co NCs revealing subtle lattice imaging of the NCs. (b) Lower-resolution TEM images of an ensemble of 10-nm hcp Co NCs.

methods allow Co NCs to be produced in several distinct crystal polymorphs with varying degrees of crystal perfection. Here we focus on two synthetic procedures that are used to prepare Co NCs with crystal structures closely related to the bulk hexagonal close-packed (hcp) and face-centered cubic (fcc) structures. A third chemical route produces Co NCs with a metastable cubic internal crystal structure, recently labeled &-Co; it has been reported in detail elsewhere [10, 19].

hcp Co NCs

High-temperature (100–300°C) reduction of metal salts in the presence of stabilizing agents has been employed to produce monodisperse Co NCs 2–12 nm in diameter. Standard air-free techniques are used. For example, in a

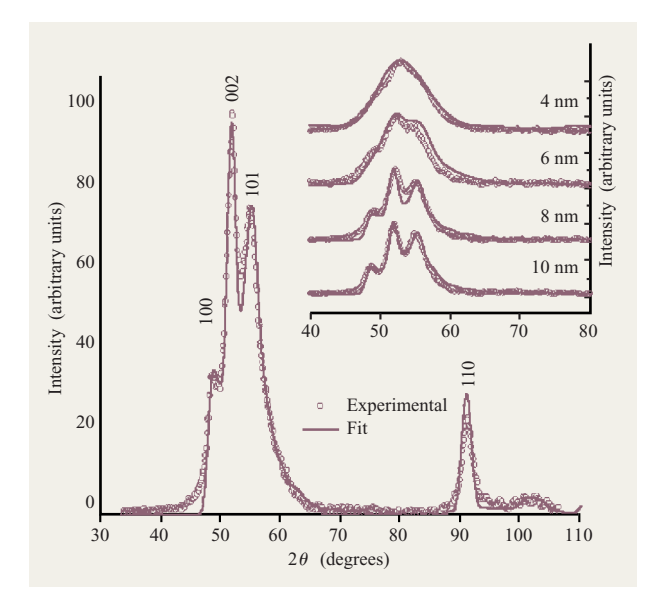


Figure 3

Wide-angle X-ray diffraction pattern of 10-nm hcp Co NCs (open circles) and computer simulation (solid curve) generated by including the statistics of size, internal structure, and shape from TEM measurements. Inset shows the WAXS patterns for a size series of hcp Co NCs, highlighting the effects of finite size broadening on the X-ray reflections.

typical reaction used to prepare 6–8-nm Co NCs, 1.0 g (4 mmol) $Co(CH_3COO)_2 \cdot 4H_2O$ is combined with 1.28 mL (4 mmol) oleic acid in a flask containing 40 mL diphenylether. The solution is heated to 200°C under a N_2 purge. As the solution is heated, H_2O is distilled out, and the purple color of the cobalt acetate tetrahydrate changes to a deep "cobalt blue." When the reaction mixture reaches 200°C, \sim 2.0 mmol trioctylphosphine is added to the solution. The bulky trioctylphosphine stabilizer provides a greater steric hindrance to the addition of cobalt species than the more compact tributylphosphine, slowing the Co NC growth rate. Tributylphosphine is substituted for trioctylphosphine in the preparation of larger NCs. The reaction mixture is then heated to 240°C.

In a separate flask, 2.1 g of a mild reducing agent, 1,2 dodecanediol (1,2 hexadecanediol may also be used) is dissolved in 10 mL of octylether and heated to 80° C. This solution is transferred using a syringe with a wide-bore needle (\sim 12 gauge) and delivered through a septum into the hot (240° C) reaction vessel. The color of the solution changes from blue to black over a period of two minutes as the Co NCs nucleate and grow. The solution is held at 240° C for \sim 10 minutes until all of the reagents are consumed. The dispersion is cooled, and ethanol is added to isolate Co NCs as an air-stable black magnetic precipitate. This preparation yields Co NC samples with a

size distribution $\sigma \sim 10\%$, which is then further narrowed by size-selective precipitation to $\sigma \sim 5\%$.

Although no Ostwald ripening is observed in this preparation, NC size is coarsely tunable by adjusting the ratio of the concentration of capping groups to that of the metal salt and by selecting the degree of bulkiness of the organophosphine stabilizer. Higher metal-to-stabilizer ratios result in larger Co NCs, while more bulky organophosphines (e.g., trioctylphosphine) favor smaller NCs.

Figure 2(a) shows a high-resolution transmission electron microscope (HRTEM) image of several ~7-nm Co NCs. Careful inspection reveals lattice spacing of \sim 2 Å, consistent with the 2.02-Å lattice spacing for the (002) planes and the 1.91-Å spacing for the (101) planes of hcp Co. Surveys of a number of such HRTEM images and electron diffraction studies indicate that the NCs are predominantly hcp but show evidence of stacking faults along the (002) axis. Lower-magnification TEM is used to image large numbers of NCs and to compile the statistics of NC size, size distribution, and shape for NC samples. A representative TEM image of ~10-nm Co NCs with a sample size distribution $\sigma \sim 6\%$ is shown in Figure 2(b). Within this TEM image, the appearance of some "darker" NCs results from enhanced diffraction contrast due to their orientation with respect to the electron beam. While there are contrast variations between the individual NCs in the sample, each NC has near-uniform contrast consistent with each NC having a single-crystal orientation and thus a single-crystalline core.

The statistical descriptions of NC sample size, shape, internal structure, and size distribution extracted from TEM images and electron diffraction patterns are used to generate an atomistic model of the NC ensemble. This model in turn is used to calculate the expected wide-angle X-ray scattering (WAXS) patterns for NC samples and can be compared with experimental diffraction patterns. The model is then refined to provide the best simultaneous fit to the TEM results and the powder X-ray diffraction measurements [9, 11]. WAXS patterns collected for hcp Co NC samples (open circles) and the corresponding computer simulations (solid curves) are shown in Figure 3. These Co NC samples are consistent with a largely hcp internal structure with fcc stacking faults along the (002) direction. The inset shows the size evolution of the X-ray diffraction patterns for hcp Co NC samples ranging in size from 4 to 10 nm in diameter. The X-ray reflections are broadened in smaller NC samples by finite size effects, and in all samples the (100), (102), and (103) reflections are further broadened and attenuated by the stacking faults along the c-axis.

Each Co NC is a single-domain magnet. Below a critical temperature (known as the blocking temperature), the magnetic moment of the NC is pinned along an "easy"

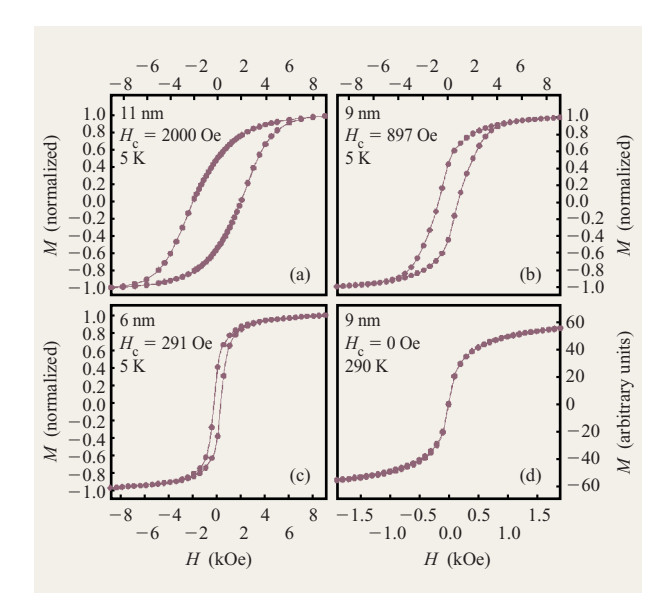


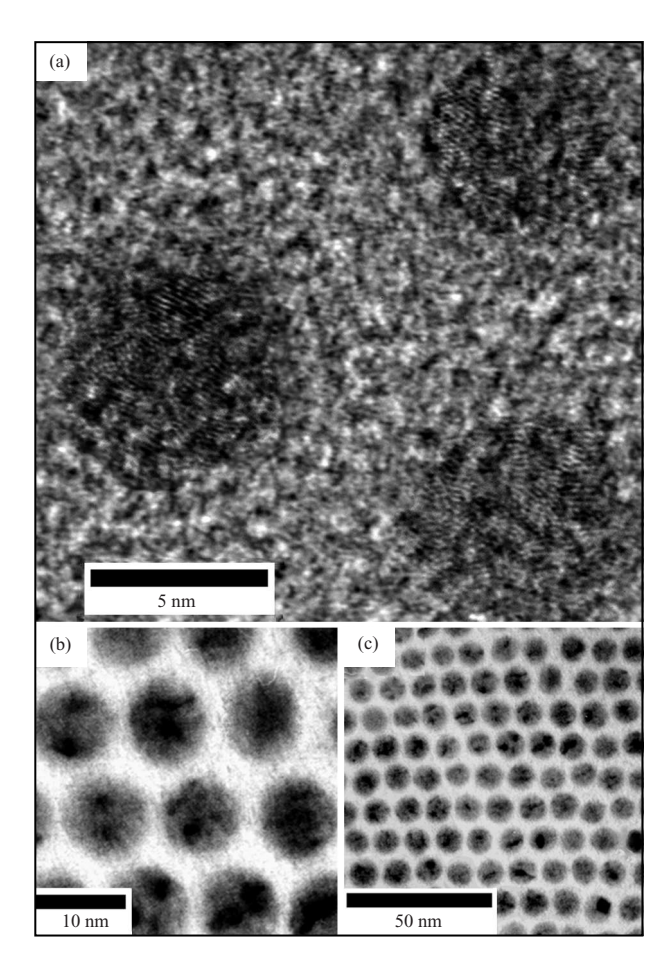
Figure 4

Magnetization versus field (*M* vs. *H*) hysteresis loops at 5 K for (a) 11-nm, (b) 9-nm, and (c) 6-nm hcp Co NC samples. Comparison of *M* vs. *H* loops for 9-nm hcp Co NCs at (b) 5 K and (d) 290 K.

axis and is said to be ferromagnetic. Above the blocking temperature, thermal fluctuations are sufficient to cause the magnetic moment to rotate between the various easy axes in the NC. This fluxional state leads to a randomization of the magnetic moments, and no hysteresis is observed.

The energetic barrier pinning the NC magnetic moment and preventing its relaxation is proportional to the product of the anisotropy constant (K) and the volume of the NC (V). The anisotropy constant includes contributions from magnetocrystalline shape and surface anisotropies. After the saturating magnetic field is removed, the magnetization, M, of an ensemble of noninteracting, single-domain NCs decays in time as $M(t) \propto e^{-t/\tau}$, where τ is exponentially proportional to KV. The double exponential dependence of M(t) on KV highlights the necessity to prepare NC samples with narrow size distributions and well-controlled crystal anisotropies to avoid significant broadening of the ferromagnetic to superparamagnetic transition.

Figures 4(a), 4(b), and **4(c)** respectively show the size-dependent *M* vs. *H* hysteresis loops at 5 K for hcp Co NCs of 11-nm, 9-nm, and 6-nm diameter. As the size of the NC decreases, the width of the hysteresis loop decreases as the energetic barrier *KV* decreases. Comparison of hysteresis loops for 9-nm hcp Co at 5 K [**Figure 4(b)**] and 290 K [**Figure 4(d)**] shows the randomization of the magnetic moments, transforming the material from ferromagnetic to superparamagnetic due to the influence of temperature.



(a) High-resolution TEM image for several 7-nm multiply twinned fcc (mt-fcc) Co NCs. (b), (c) Low-resolution TEM images of ensembles of 9-nm mt-fcc Co NCs. Note the contrast variations within an individual NC in the image (see description in text).

Multiply twinned FCC Co NCs

A second polymorph of Co NCs, in which each NC comprises multiple fragments of the bulk fcc lattice, may be prepared by thermal decomposition of cobalt octacarbonyl [Co₂(CO)₈] in the presence of stabilizing ligands. Variations on this procedure have been known for years to produce metal NCs when oxygen is excluded from the reaction [20], and to prepare metal oxide NCs when oxygen/air is introduced during the reaction [21, 22]. We report a refined synthesis using Co₂(CO)₈ as a precursor to prepare multiply twinned fcc (mt-fcc) Co NC samples with narrow size distributions. Standard air-free handling procedures are again employed until the NC growth is complete. In a typical synthesis for ~8- to 10-nm mt-fcc Co, a reaction vessel containing 30 mL diphenylether (one could use octylether, but it is significantly more costly), 2 mmol (0.64 mL) oleic acid, and 2.0 mmol

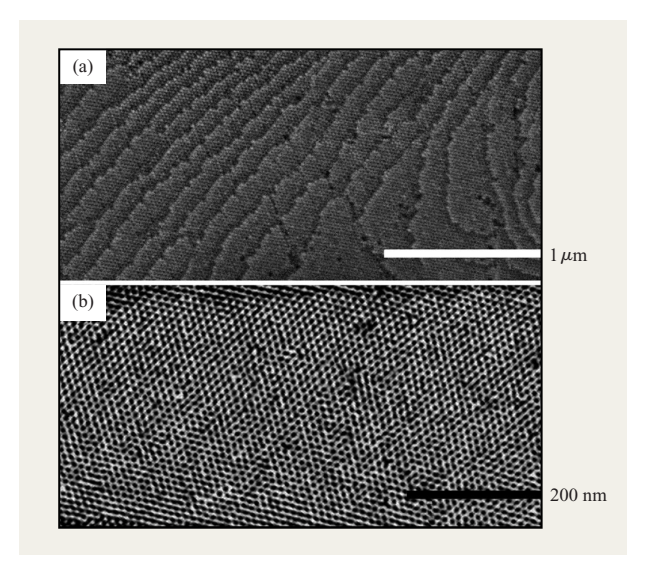


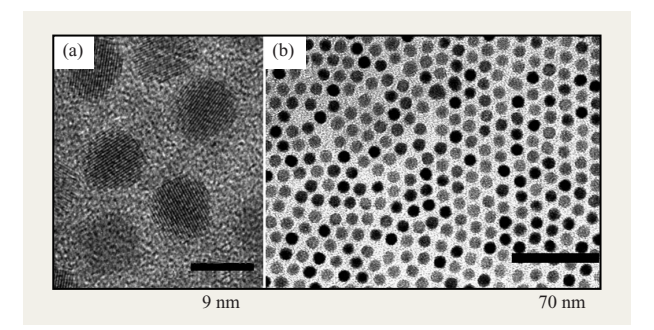
Figure 6

(a) High-resolution scanning electron micrograph of a 10-nm Co NC superlattice. (b) Low-resolution TEM image of an 8-nm Co NC superlattice.

tributylphosphine is heated under a N_2 flush to 200°C . In a separate flask, 684 mg $\text{Co}_2(\text{CO})_8$ is combined with 10 mL dioctylether, warmed to 60°C under a flush of N_2 , and stirred until fully dissolved. The $\text{Co}_2(\text{CO})_8$ solution in dioctylether is viscous and is therefore transferred in a syringe with a wide-bore needle (~12 gauge). The solution is rapidly injected through a septum into the hot vessel (200°C) containing the diphenylether solvent and the oleic acid and organophosphine stabilizers. Upon injection, the solution turns black in color and bubbles as $\text{Co}_2(\text{CO})_8$ decomposes, nucleating Co NCs and releasing CO gas. This solution is then heated at 200°C for ~15 minutes and vigorously stirred. The NC dispersion is cooled to room temperature, and the NCs are isolated from solution as described above for hcp Co NC samples.

Figure 5 shows high- and low-resolution TEM images of the mt-fcc NC samples. HRTEM images, as shown in Figure 5(a) for several ~7-nm NCs, reveal complicated interference patterns at a resolution sufficient to image the lattice. The patterns are consistent with multiple crystal orientations contained within a single NC [23]. This is also seen in lower-resolution TEM images, as shown in Figures 5(b) and 5(c). The contrast variations within each NC arise because lattice fragments are at different orientations with respect to the electron beam.

More detailed magnetic studies of these multiply twinned NCs will allow comparison with size-dependent trends in better-crystallized hcp and ϵ -Co NC samples. These studies will highlight the importance of internal



TEM micrographs of PbSe (a) at high resolution, revealing lattice imaging of the NCs; (b) at low resolution, showing an ensemble of NCs.

crystal structure on the magnetic properties of nanocrystalline material.

The narrow size distribution of NC samples prepared by this synthetic route allows these NCs to self-assemble from solution into ordered arrays. For example, superlattices of oleic-acid-capped Co NCs are deposited by dispersing the NC sample in either hexane or a mixture of hexane and octane, depositing the NC dispersion on a substrate surface, and covering the solution/substrate with a petri dish to slow the rate of solvent evaporation. Slowing the rate of solvent evaporation allows sufficient time for NCs from solution and on the surface to find equilibrium lattice sites on the growing NC superlattice. Figure 6(a) shows a high-resolution scanning electron microscope (HRSEM) image of a NC superlattice composed of 10-nm mt-fcc Co NCs. Well-ordered terraces, ledges, and kinks are apparent as NCs add to the growing superlattice, much like atoms on a growing crystal surface. Lowresolution TEM imaging [Figure 6(b)] shows a projection of a superlattice formed from 8-nm Co NCs.

Nanocrystal semiconductors—PbSe NCs (quantum dots)

PbSe NCs are synthesized by rapidly injecting a room-temperature solution of lead oleate and trioctylphosphine selenide dissolved in trioctylphosphine into a rapidly stirred solution containing diphenylether at 150°C.¹ Upon injection, small (<2-nm) PbSe NCs nucleate and begin to grow, even as the solution temperature drops toward 80°C because of the addition of the room-temperature reagents. Raising the solution temperature accelerates the NC growth rate, and higher temperatures are used to prepare large-size NCs. Solution temperatures of 90 to 220°C are used to tune the size of PbSe NC samples from 3.5 nm to

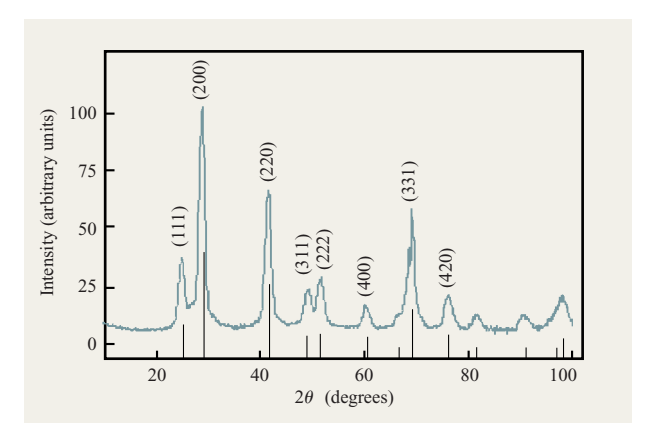


Figure 8

Wide-angle X-ray diffraction pattern of 10-nm PbSe NCs indexed to the bulk rock-salt crystal structure.

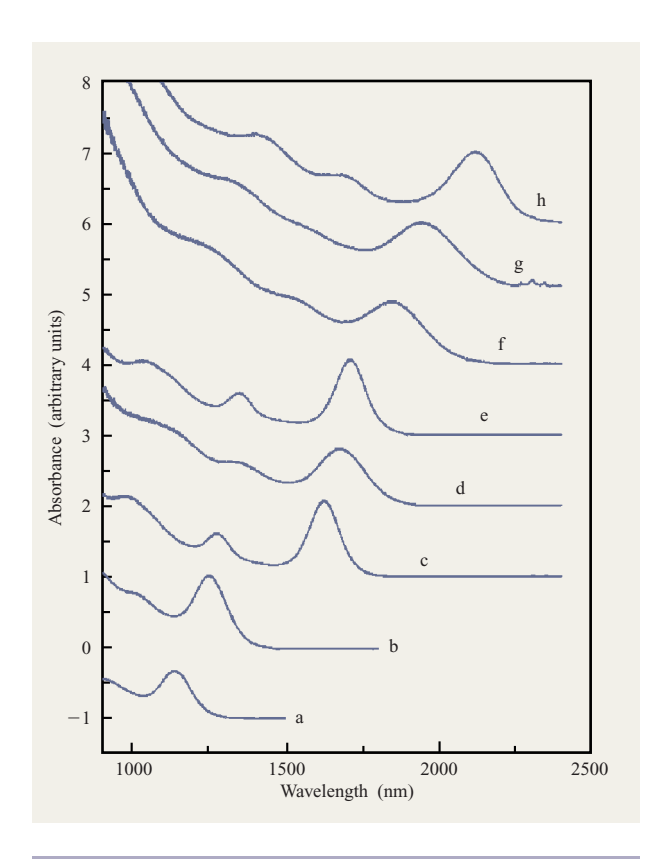


Figure 9

Room-temperature optical absorption spectra for a series of PbSe NC samples measuring (a) 3.0 nm, (b) 3.5 nm, (c) 4.5 nm, (d) 5 nm, (e) 5.5 nm, (f) 7 nm, (g) 8 nm, and (h) 9 nm in diameter.

15 nm in diameter. PbSe NC samples can be isolated from solution within \sim 15 minutes of the precursor injection.

¹ W. Gaschler and C. B. Murray, "Synthesis of Lead Selenide Nanocrystals: Quantum Cubes and Quantum Spheres," work in preparation.

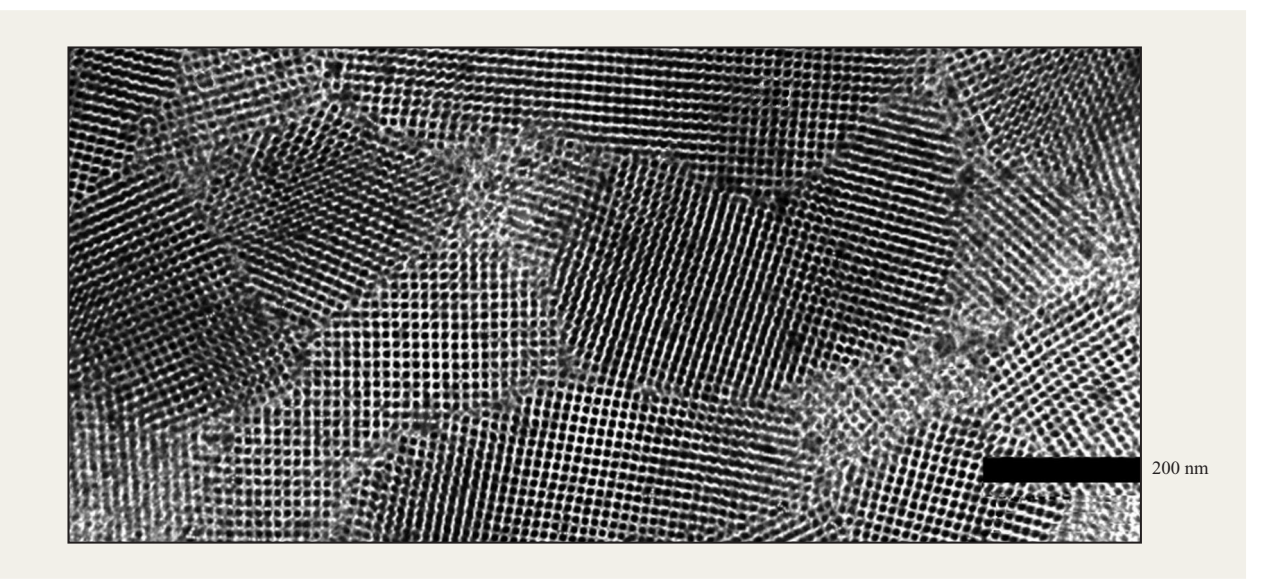


Figure 10

TEM micrograph of a superlattice of 8-nm PbSe NCs.

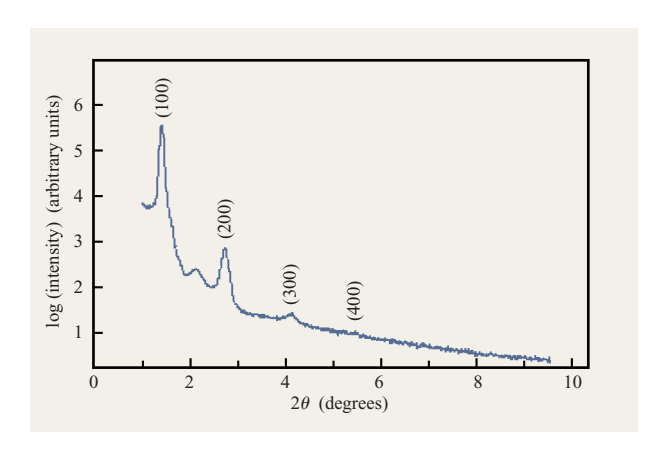


Figure 11

Small-angle X-ray scattering of an 8-nm PbSe NC superlattice indexed to a simple cubic structure.

After the PbSe NCs reach the desired size, the dispersion is cooled and short-chain alcohols are added to flocculate the NCs, which are then separated from solution by centrifuging. The NC size distribution $\sigma \sim 10\%$ is further narrowed by size-selective precipitation to 5% or better. Figure 7(a) shows a high-resolution TEM image of ~8-nm PbSe NCs. The internal crystal lattice is clearly resolved in several NCs. Lower-magnification imaging [Figure 7(b)] shows the consistent size and shape of the PbSe NCs within a sample. As the surface coverage

of NCs approaches one monolayer, these uniform NC samples begin to be ordered into close-packed assemblies. WAXS patterns for 10-nm PbSe NCs [Figure 8) match the bulk rock-salt structure (bulk reflections indicated as lines from the 2θ axis). TEM images and X-ray diffraction patterns show that the individual PbSe NCs are single crystals of the bulk rock-salt lattice and show no signs of faulting.

Semiconductor NCs smaller in size than the bulk exciton Bohr radius confine electronic excitations in all three dimensions. Three-dimensional confinement effects collapse the continuous density of states of the bulk solid into the discrete electronic states of the NC. For PbSe, the bulk Bohr radius is 46 nm. In **Figure 9**, optical absorption spectra for a size series of PbSe NC samples, ranging in size from 3.0 nm to 9 nm in diameter, show the expected size-dependent effects of quantum confinement. As the NC diameter decreases, the absorption edge shifts to the blue, and the separation between electronic transitions increases.

Figure 10 shows a TEM image of a three-dimensional superlattice of oleic-acid-capped 8-nm PbSe NCs. The PbSe NCs pack in a simple cubic lattice with the long organic ligands filling the interstices between NCs in the superlattice. In this image a number of ordered domains have nucleated simultaneously and have grown together, providing a mosaic texture to the thin film. Small-angle X-ray scattering (SAXS) measurements, as shown in Figure 11, reveal reflections arising from the scattering of X-rays off the planes of the NC superlattice [9, 12].

Indexing of the reflections in the SAXS pattern is consistent with the simple cubic NC superlattice imaged in TEM and shows that the NC superlattice is preferentially (100)-oriented with respect to the substrate surface.

Conclusion

High-temperature solution-phase syntheses yield magnetic and semiconductor NC samples that are uniform in size to \pm one atomic layer, composition, shape, internal structure, and surface chemistry. Systematic study of a series of NC sizes permits the size-dependent electronic, magnetic, and optical properties of nanometer-size materials to be mapped. Under controlled deposition conditions, NC samples that are sufficiently uniform in size self-assemble from solutions to form ordered NC arrays. The size and composition of the NCs and the length and chemical functionality of the organic capping layer can be tailored to engineer the physical properties of NC superlattices.

Acknowledgments

Dr. Gaschler's research was supported by the Defense Advanced Research Projects Agency through ARO Grant No. DAAD19-99-1-0001.

References

- E. C. Stoner and E. P. Wohlfarth, "A Mechanism of Magnetic Hysteresis in Heterogeneous Alloys," *Phil. Trans. Roy. Soc. A* 240, 599-642 (1948).
- F. E. Luborsky, "Development of Elongated Particle Magnets," J. Appl. Phys. 32, 1715–183S (1961).
- A. Aharoni, Introduction to the Theory of Ferromagnetism, Oxford University Press, New York, 1996, pp. 133–152.
- S. Morup, "Studies of Superparamagnetism in Samples of Ultrafine Particles," *Nanomagnetism*, A. Hernando, Ed., Kluwer Academic Publishers, Boston, 1993, pp. 93–99.
- S. Sun, C. B. Murray, D. Weller, L. Folks, and A. Moser, "Monodisperse FePt Nanoparticles and Ferromagnetic Nanocrystal Superlattices," Science 287, 1989-1992 (2000).
 S. V. Gaponenko, Optical Properties of Semiconductor
- S. V. Gaponenko, Optical Properties of Semiconductor Nanocrystals, Cambridge University Press, Cambridge, England, 1998.
- 7. U. Woggon, Optical Properties of Semiconductor Quantum Dots, Springer-Verlag, Berlin, 1997.
- 8. A. P. Alivisatos, "Semiconductor Clusters, Nanocrystals, and Quantum Dots," *Science* **271**, 933–937 (1996).
- C. B. Murray, C. R. Kagan, and M. G. Bawendi, "Synthesis and Characterization of Monodisperse Nanocrystals and Close-Packed Nanocrystal Assemblies," Ann. Rev. Mater. Sci. 30, 545-610 (2000).
- S. Sun, C. B. Murray, and H. Doyle, "Controlled Assembly of Monodisperse ε-Cobalt-Based Nanocrystals," Mater. Res. Soc. Symp. Proc. 577, 385–398 (1999).
- C. B. Murray, D. J. Norris, and M. G. Bawendi, "Synthesis and Characterization of Nearly Monodisperse CdE (E = S, Se, Te) Semiconductor Nanocrystallites," *J. Amer. Chem. Soc.* 115, 8706–8715 (1993).
- C. B. Murray, C. R. Kagan, and M. G. Bawendi, "Self-Organization of Close-Packed Quantum Dot Solids for CdSe Nanocrystallites," *Science* 270, 1335–1338 (1995).
- 13. C. R. Kagan, C. B. Murray, and M. G. Bawendi, "Long-Range Resonance Transfer of Electronic Excitations in Close-Packed CdSe Quantum-Dot Solids," *Phys. Rev. B* **54**, 8633–8643 (1996).

- C. P. Collier, R. J. Saykally, J. J. Shang, S. E. Henrichs, and J. R. Heath, "Reversible Tuning of Silver Quantum Dot Monolayers Through the Metal Insulator Transition," *Science* 277, 1978–1981 (1997).
- X. Peng, J. Wickham, and A. P. Alivisatos, "Kinetics of II–VI and III–V Colloidal Semiconductor Nanocrystal Growth: 'Focusing' of Size Distributions," *J. Amer. Chem.* Soc. 120, 5343–5344 (1998).
- 16. A. Chemseddine and H. Weller, "Highly Monodisperse Quantum Sized CdS Particles by Size Selective Precipitation," *Ber. Bunsen-Ges. Phys. Chem.* **97**, 636–637 (1993).
- C. T. Black, C. B. Murray, R. L. Sandstrom, and Shouheng Sun, "Spin-Dependent Tunneling in Self-Assembled Cobalt Nanocrystal Superlattices," *Science* 290, 1131–1134 (2000).
- For an extensive review, see G. Schmid, Clusters and Colloids: From Theory to Applications, John Wiley & Sons, Inc., New York, 1994.
- D. P. Dinega and M. G. Bawendi, "A Solution-Phase Chemical Approach to a New Crystal Structure of Cobalt," *Angew. Chem.* 38, 1788 (1999).
- E. Blums, A. Cebers, and M. M. Maiorov, "Preparation of Magnetic Fluids by Decomposing Carbonyls and Other Compounds," *Magnetic Fluids*, Walter de Gruyter and Co., Berlin, 1996, pp. 347–351.
- 21. M. D. Bentzon, J. van Wonterghem, S. Mørup, and A. Thölén, "Ordered Aggregates of Ultrafine Iron Oxide Particles: 'Super Crystals,'" *Phil. Mag. B* **60**, 169–178 (1989).
- J. S. Yin and Z. L. Wang, "In Situ Structural Evolution of Self-Assembled Oxide Nanocrystals," *J. Phys. Chem. B* 101, 8979–8983 (1997).
- 23. L. D. Marks, "Experimental Studies of Small Particle Structures," *Rep. Prog. Phys.* **57**, 603–649 (1994).

Received December 5, 2000; accepted for publication January 5, 2001

Christopher B. Murray IBM Research Division, Thomas J. Watson Research Center, P.O. Box 218, Yorktown Heights, New York 10598 (cbmurray@us.ibm.com). Dr. Murray is the manager of the Nanoscale Materials and Devices Department and contributes to the preparation and characterization of nanoscale materials. He joined IBM in 1995 after completing his Ph.D. studies in chemistry at MIT.

Shouheng Sun IBM Research Division, Thomas J. Watson Research Center, P.O. Box 218, Yorktown Heights, New York 10598 (ssun@us.ibm.com). Dr. Sun is a materials chemist who has developed leading synthetic routes for the preparation of monodisperse magnetic nanostructures. He joined IBM in 1996 after completing his Ph.D. studies in chemistry at Brown University.

Wolfgang Gaschler BASF AG, Akiengesellschaft, ZkD-B001, Germany (Wolfgang.Gaschler@basf-ag.de). Dr. Gaschler was a visiting scientist at the IBM Thomas J. Watson Research Center from 1999 to 2000. He carried out studies on semiconductor nanocrystal superlattices in collaboration with the Advanced Materials Research Institute (AMRI) at the University of New Orleans, Louisiana.

Hugh Doyle National Microelectronics Research Center, University College Cork, Lee Naltings, Cork, Ireland (hugh_doyle@hotmail.com). Dr. Doyle was a visiting scientist at the IBM Thomas J. Watson Research Center from 1998 to 2000 developing computational models of nanoscale structures. He joined IBM in 1998 after completing his Ph.D. studies in chemistry at the University College of Dublin, Ireland.

Theodore A. Betley California Institute of Technology, Division of Chemistry and Chemical Engineering, 1200 E. California Blvd., Pasadena, California 91125 (betley@its.caltech.edu). In 1999 Mr. Betley worked as a summer intern at the IBM Thomas J. Watson Research Center in Yorktown Heights, New York, contributing to the synthesis of monodisperse magnetic nanocrystals. In 2000, upon completing his bachelor's degree in chemical engineering at the University of Michigan, Mr. Betley began his graduate studies in chemistry at the California Institute of Technology.

Cherie R. Kagan IBM Research Division, Thomas J. Watson Research Center, P.O. Box 218, Yorktown Heights, New York 10598 (cheriek@us.ibm.com). Dr. Kagan is a Research Staff Member in the Physical Sciences Department at the IBM Thomas J. Watson Research Center. She received a B.S.E. degree in materials science and engineering and a B.A. degree in mathematics, both from the University of Pennsylvania, in 1991. In 1996, she received her Ph.D. degree in electronic materials from MIT. Her thesis work focused on the selfassembly of close-packed solids of semiconductor nanocrystals and the unique electronic and optical properties that arise from cooperative interactions between neighboring nanocrystals. In 1996, Dr. Kagan went as a Postdoctoral Fellow to Bell Laboratories, where she built a scanning confocal Raman microscope to study the formation of holograms in multicomponent photopolymers. In 1998 she joined IBM, where she has been investigating the optical and electrical properties of organic-inorganic hybrid materials and the application and patterning of organic-inorganic hybrids and soluble organic semiconductors in thin-film field-effect transistors.

56